Nuclear Engineering and Technology 53 (2021) 1277–1283

Contents lists available at ScienceDirect

Nuclear Engineering and Technology

journal homepage: www.elsevier.com/locate/net

Original Article

Proposing a gamma radiation based intelligent system for simultaneous analyzing and detecting type and amount of petroleum by-products

Mohammadmehdi Roshani [a, b], Giang Phan [a], Rezhna Hassan Faraj [c], Nhut-Huan Phan [a], Gholam Hossein Roshani [d], Behrooz Nazemi [e], Enrico Corniani [f, g, *], Ehsan Nazemi [h]

[a] Institute of Fundamental and Applied Sciences, Duy Tan University, Ho Chi Minh City, Viet Nam
[b] Faculty of Electrical – Electronic Engineering, Duy Tan University, Da Nang, 550000, Viet Nam
[c] Department of Chemistry, Faculty of Science and Health, Koya University, Koya, KOY45, Kurdistan Region, Iraq
[d] Electrical Engineering Department, Kermanshah University of Technology, Kermanshah, Iran
[e] Faculty of Art and Architecture, Yazd University, Yazd, Iran
[f] Division of Nuclear Physics, Advanced Institute of Materials Science, Ton Duc Thang University, Ho Chi Minh City, Viet Nam
[g] Faculty of Applied Sciences, Ton Duc Thang University, Ho Chi Minh City, Viet Nam
[h] Imec-Vision Lab, Department of Physics, University of Antwerp, Antwerp, Belgium

ARTICLE INFO

Article history:
Received 24 May 2020
Received in revised form
18 August 2020
Accepted 14 September 2020
Available online 16 September 2020

Keywords:
Petroleum by-products
Artificial intelligence
Online monitoring
Dual energy source
Poly-pipelines

ABSTRACT

It is important for operators of poly-pipelines in petroleum industry to continuously monitor characteristics of transferred fluid such as its type and amount. To achieve this aim, in this study a dual energy gamma attenuation technique in combination with artificial neural network (ANN) is proposed to simultaneously determine type and amount of four different petroleum by-products. The detection system is composed of a dual energy gamma source, including americium-241 and barium-133 radioisotopes, and one 2.54 cm × 2.54 cm sodium iodide detector for recording the transmitted photons. Two signals recorded in transmission detector, namely the counts under photo peak of Americium-241 with energy of 59.5 keV and the counts under photo peak of Barium-133 with energy of 356 keV, were applied to the ANN as the two inputs and volume percentages of petroleum by-products were assigned as the outputs.

1. Introduction

In petrochemical and petroleum industries, a same pipeline, so called poly-pipelines, is usually implemented for transporting more than one product. In such situations, it is important for operators of pipeline to continuously monitor characteristics of transferred fluid such as its type, amount, and etc. In poly-pipelines, once for a defined time interval the piping product changes, the two products will be in contact with each other and consequently contamination (mixing) is happened which defines an interface region between the two products. During the interface, the mixed fluid must be directed to special tanks or to a separation unit, that leads to increasing economic costs. This situation highlights the necessity of developing nondestructive techniques to precisely identify the fluid interface region with the aim of optimizing transportation in a poly-pipeline [1].

It has been proved that photon attenuation based techniques can serve as a potential nondestructive technique for measuring different properties of fluids in petroleum and petrochemical industries [2–13]. In regard of using gamma radiation based techniques for monitoring petroleum's product, some investigations have been carried out in past years. In 2011, M. Khorsandi et al., performed a Monte Carlo simulation based study to evaluate the sensitivity of two main gamma radiation based techniques, namely transmission and scattering, for measuring the density of petroleum products [14]. They indicated that the sensitivity of gamma transmission technique is more than scattering one. After that, they designed an experimental setup, composed of a cesium-137 disk source with an activity of 1.85×10^6 Bq and one 7.62 cm sodium iodide crystal detector, to measure density of some oil products

* Corresponding author. Division of Nuclear Physics, Advanced Institute of Materials Science, Ton Duc Thang University, Ho Chi Minh City, Viet Nam.
E-mail address: enrico.corniani@tdtu.edu.vn (E. Corniani).

https://doi.org/10.1016/j.net.2020.09.015

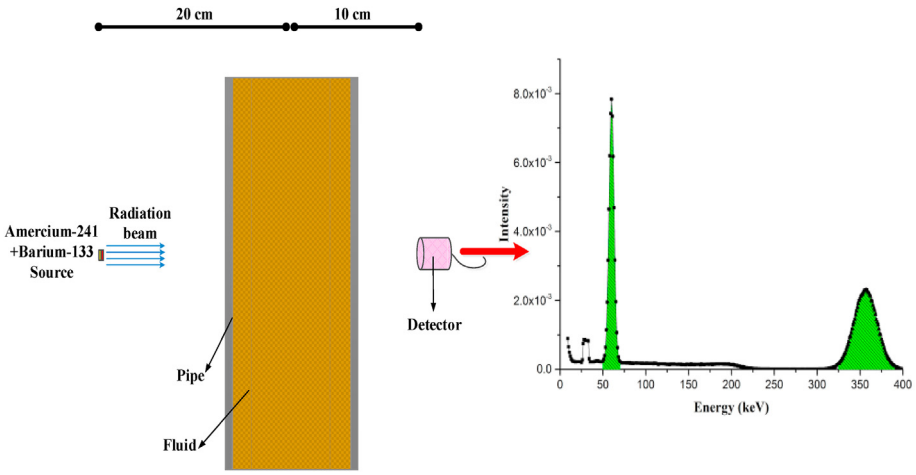

Fig. 1. Configuration of simulated detection system and recorded signals from the detector.

Table 1
The calculated constant parameters for GEB option [21].

Parameter	a	b	c
Value (unit)	1.09×10^{-2} (MeV)	6.96×10^{-2} ($MeV^{0.5}$)	2.26×10^{-2} (MeV^{-1})

such as gasoil, gasoline, and etc. using gamma transmission technique. In 2013, G. H. Roshani et al., proposed an approach to estimate density of some petroleum derivatives independent of pipe's diameter [15]. The proposed methodology included combination of adaptive neuro-fuzzy inference system (ANFIS) technique and a single gamma-ray densitometer. The detection system was composed of a polyethylene pipe with a diameter of 10.16 cm, a cesium-137 radioisotope, and one 7.62 cm sodium iodide crystal detector. The pipe diameter and registered count in the detector were assigned as the two inputs of ANFIS and the density was used as the output. Implementing this technique, they succeeded to estimate the density independent of pipe's diameter with an error of less than 2.64%. In 2016, C. Salgado et al. proposed a method included combination of a broad beam detection system and artificial neural network (ANN) for estimating density of petroleum and derivatives [1]. The detection system included a cesium-137 radioisotope and one sodium iodide crystal detector. Using MCNPX code, they modelled various petroleum products with densities in the range of 0.55–1.26 g/cm^3. The recorded photon energy spectrum in the detector was used as input of ANN. Using this methodology, density of petroleum products was estimated independent of their material composition. In 2020, W. L. Salgado et al. established an experimental setup to validate the Monte Carlo simulation carried out to investigate identifying the interface region [16]. The experimental setup was composed of a cesium-137 radioisotope, a glass pipe, and one sodium iodide crystal detector. Inside the pipe, stratified flow regime was modelled. Two liquids, namely lubricating oil and water, with different percentages were utilized in the experiments. Applying this method, they succeeded to determine the region interface with an accuracy of 1%.

As pointed out in the literature review, in former studies the researchers mainly concentrated on measuring of one property of petroleum products such as density or volume fraction supposing the type of product is known. But in a real situation, operator of poly-pipeline doesn't have any prior knowledge about the type and amount of transferring product. So, in this study an intelligent and online system with the ability of detecting type and amount of transferring fluid is proposed to cover the gap. The proposed methodology includes a dual energy gamma attenuation technique in combination with ANN.

2. Methodology

2.1. Monte Carlo simulation

As mentioned previously, the main objective of current work is online measuring type and amount of fluid in oil industry's transfer poly-pipelines. A conventional single energy gamma radiation based instrument that works based on Beer–Lambert's law and includes one radiation source and one detector, can just measure the amount of a material located between radiation source and detector when its type is known, and vice versa. In regards of our problem in this work, there are two unknown, namely type of fluid and its amount. So, at least two known signals are required. In this investigation Monte Carlo N-Particle code version X (MCNP-X) [17] was used to evaluate the idea of adopting a dual energy gamma source and one sodium iodide detector for resolving the mentioned problem. The proposed detection system is composed of a dual energy gamma source, including americium-241 and barium-133 radioisotopes, and one 25.4 × 25.4 mm sodium iodide crystal detector. The reason for choosing mentioned radioisotopes is that americium-241 emits low energy photons (59.5 keV) while barium-133 emits relatively high energy photons (356 keV). The emitted photons from aforementioned radioisotopes interact with medium

Table 2
Specifications of four kinds of oil by-products considered as the fluid in the pipe in this study.

No./Oil by-product	Name	Chemical formula	Density (g/cm3)
1	Ethylene Glycol	C2H6O2	1.114
2	Crude oil (Heavy, Mexican)	–	0.975
3	Gasoil	C12H23	0.826
4	Gasoline	C8H18	0.721

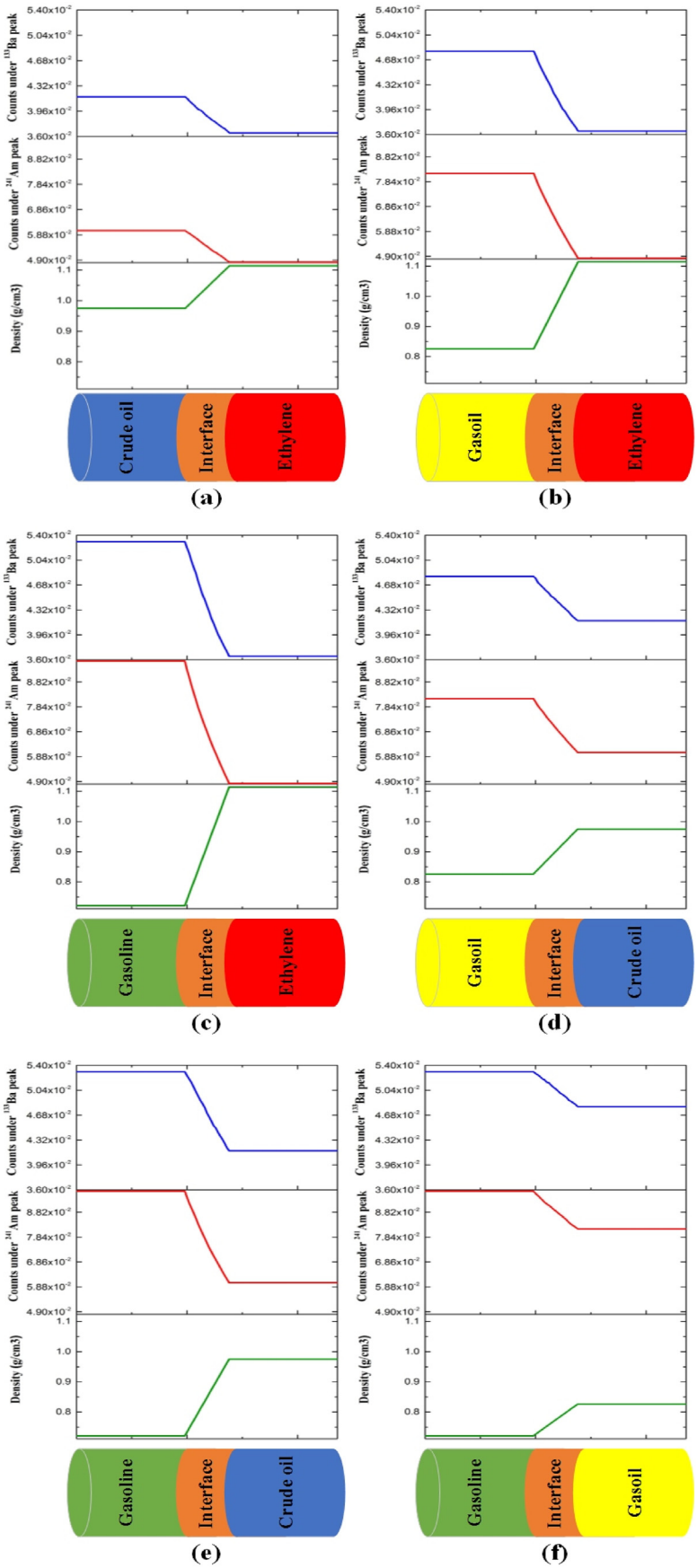

Fig. 2. The recorded counts under photo peaks of americium-241 and barium-133 as well as density of each simulated mixture for six different possible interface states: 1- Ethylene Glycol and crude oil, 2- Ethylene Glycol and gasoil, 3- Ethylene Glycol and gasoline, 4- Crude oil and gasoil, 5- Crude oil and gasoline, and 6- Gasoil and gasoline.

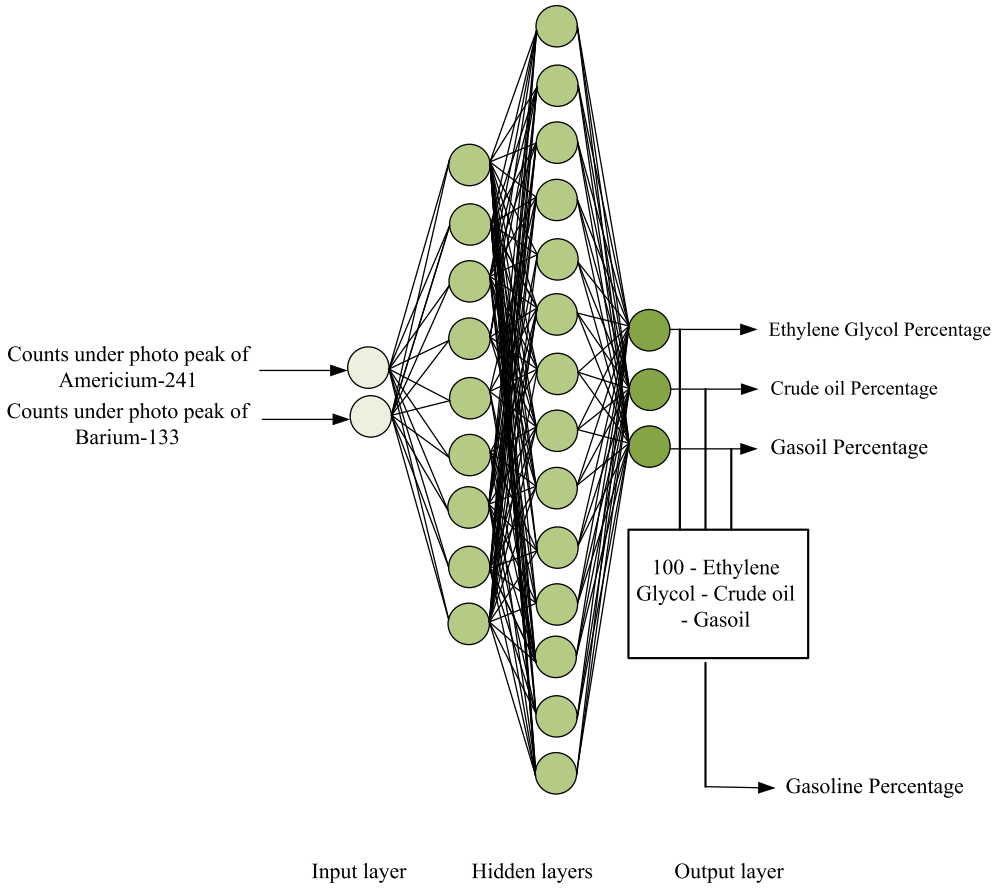

Fig. 3. Architecture of proposed network in order to determine type and amount of petroleum products.

via two main different mechanism, namely photoelectric and Campton scattering. Indeed, photoelectric is dominant interaction mechanism for low energy photons, while Campton scattering is dominant interaction mechanism for high energy photons. Having photons with different interaction mechanisms, the recognition of material's properties can be determined better. The simulation configuration is indicated in Fig. 1. It is good to note that the performance of current simulated detection system was validated with an established experimental setup proposed in our former works [18–20].

As it is shown in Fig. 1, the detector was located in front of the dual energy radiation source at a distance of 30 cm from the pipe. Pulse height tally (tally type F8) was used to record photon energy spectrum in the detector. In each simulation, counts under photo peaks of americium-241 and barium-133 with gamma energies of 59.5 keV and 356 keV were registered to provide sufficient dataset for training and testing the ANN. Gaussian energy broadening (GEB) option was also implemented in this work to take the energy broadening of photon spectrum into account in the simulated sodium iodide crystal detector. The required constant parameters for this option were calculated in our former work [21]. The mentioned parameters (the values are shown in Table 1) were inserted into "FT8 GEB" card.

In order to decrease the computing time, a collimated dual energy source was defined instead of an isotropic one. To do this aim, DIR and VEC options in the source definition (SDEF) card of MCNPX's input file were implemented.

A Pyrex-glass pipe with an external diameter and thickness of 10 cm and 0.25 cm was defined in simulations as the main pipe. In this study, four kinds of oil by-products were considered as the fluid in the pipe. The required information about composition of used materials were obtained from Refs. [22]. The specifications of considered fluids are shown in Table 2.

Since in a poly-pipeline two various fluids are in direct contact with each other, fluid contamination is happened which defines an interface region. In this work, we modelled the interface region between each two fluids. In the case of considered four fluids, as shown in Fig. 2, six possible interface regions can be occurred: 1- Ethylene Glycol and crude oil, 2- Ethylene Glycol and gasoil, 3- Ethylene Glycol and gasoline, 4- Crude oil and gasoil, 5- Crude oil and gasoline, and 6- Gasoil and gasoline. In fact, the interface region is a mixture of two fluids that are in contact with each other. In this region, the amount of first fluid is gradually decreased when move toward the second one. To model interface region, a mixture of two fluids for six possible states were considered. The mixture includes 5–95% from each fluid as a complementary. The recorded counts under photo peaks of americium-241 and barium-133 as well as density of each simulated mixture are shown in Fig. 2 for six different states. In this investigation, totally 118 simulations were carried out (6 different interface region $\times$ 19 different mixture combinations+4 single fluids = 118).

2.2. Artificial neural network (ANN)

Today multi-layer perceptron (MLP) is still the most popular and the most widespread kind of neural network. MLP is a strong tool for modeling different problems and it has very good and proofed approximation capabilities. In this kind of neural network there are

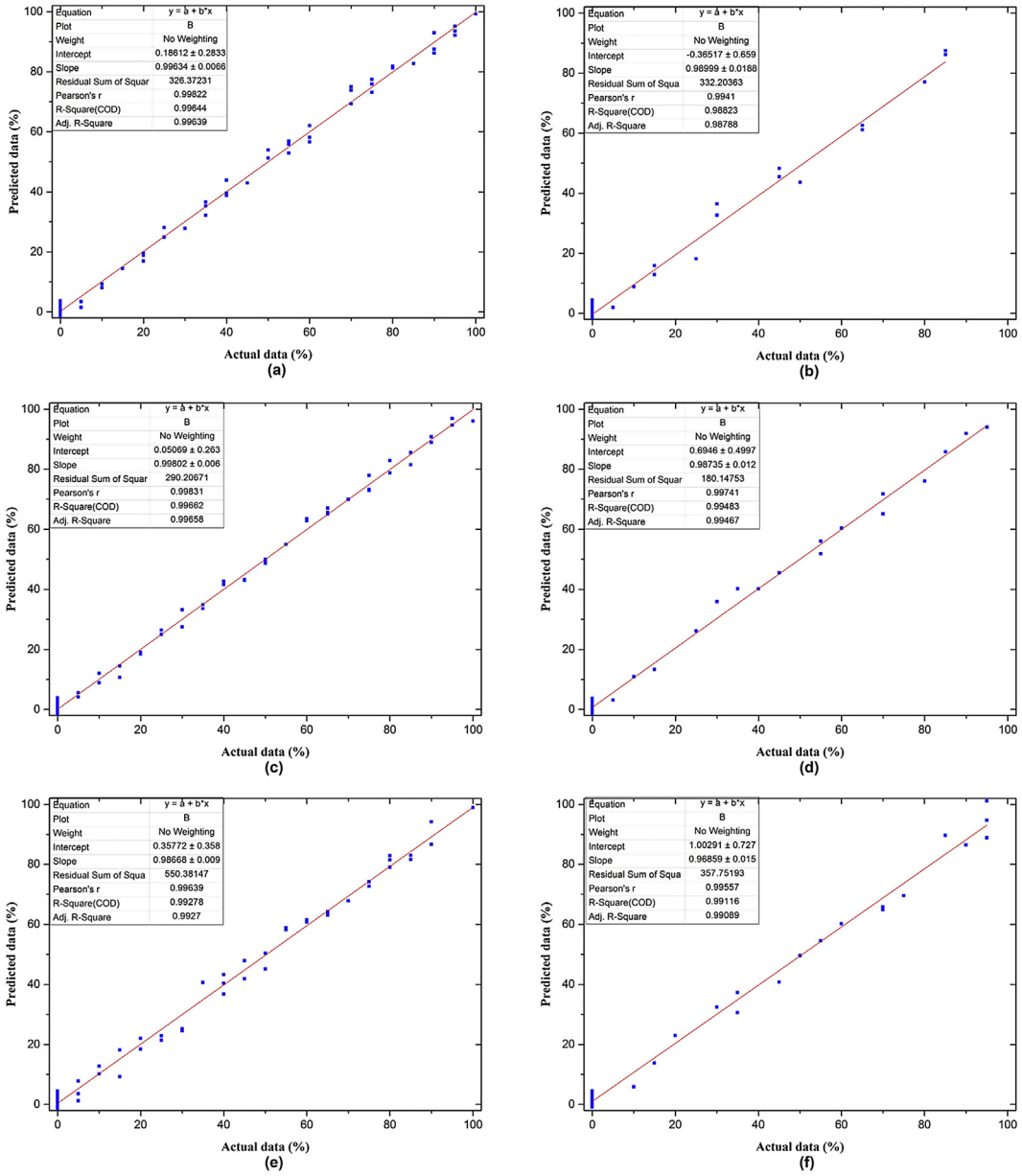

Fig. 4. Regression diagrams of actual and estimated results for a) train data - Ethylene Glycol b) test data - Ethylene Glycol c) train data – Crude oil d) test data – Crude oil e) train data - Gasoil f) test data - Gasoil.

several methods for finding the weighs and biases. Levenberg Marquardt (LM) algorithm has been implemented for training the presented network. The LM algorithm which is the most widely used optimization algorithm is a combination of Gauss-Newton method and gradient descent [22].

In this study, a MLP-LM network with two inputs and three outputs was considered. Two features were extracted from detectors output signals and were regarded as MLP-LM inputs. The Architecture of proposed network in order to determine type and amount of petroleum products was illustrated in Fig. 3. The trained network can meter the percentages of Ethylene Glycol, Crude oil and gasoil based on input signals, precisely. The percentage of remained material (gasoline) can be obtained simply by subtracting other percentages from 100.

In the Monte Carlo simulations, 108 various cases were modelled. 83 cases were implemented for training and 35 cases were utilized for testing the efficiency of presented network. To find the optimized architecture of MLP-LM network, several different architectures were examined in several loops based on presented algorithm. The presented algorithm is:

1) The data set including train and test data was defined.
2) The data set was normalized.
3) The counters were defined.
4) The initial values for different parameters were set.
5) Several nested loops were created in order to optimize the structure.
6) The error was defined.
7) Different number of hidden layers, different number of neurons in each layer, different epochs and different activation functions for several times were tested using the defined counters and parameters initial values.

Table 3
The test data with predicted values.

Test Data										
Data No.	Counts under photo peak of Americium-241	Counts under photo peak of Barium-133	Actual Percentage of Ethylene Glycol	Actual Percentage of Crude oil	Actual Percentage of Gasoil	Actual Percentage of Gasoline	Predicted Percentage of Ethylene Glycol	Predicted Percentage of Crude oil	Predicted Percentage of Gasoil	Predicted Percentage of Gasoline
1	9.64E-02	5.31E-02	0	0	0	100	−1.4	−0.41	3.48	98.40
2	5.87E-02	4.07E-02	15	85	0	0	12.90	85.75	1.97	−0.63
3	5.68E-02	3.98E-02	30	70	0	0	36.43	65.07	2.26	−3.77
4	5.48E-02	3.91E-02	45	55	0	0	48.22	51.81	0.71	−0.75
5	5.23E-02	3.82E-02	65	35	0	0	61.09	40.18	3.18	−4.46
6	5.02E-02	3.73E-02	85	15	0	0	86.14	13.32	−0.95	1.48
7	7.95E-02	4.73E-02	5	0	95	0	1.90	3.74	101.10	−6.74
8	7.54E-02	4.58E-02	15	0	85	0	15.86	−2.68	89.61	−2.79
9	6.99E-02	4.39E-02	30	0	70	0	32.65	1.47	65.87	0.00
10	6.32E-02	4.15E-02	50	0	50	0	43.61	2.26	49.54	4.57
11	5.86E-02	3.98E-02	65	0	35	0	62.56	−0.95	37.25	1.13
12	5.25E-02	3.79E-02	85	0	15	0	87.47	3.25	13.80	−4.53
13	9.00E-02	5.13E-02	10	0	0	90	8.84	3.23	2.83	85.09
14	8.11E-02	4.85E-02	25	0	0	75	18.17	0.10	0.01	81.69
15	7.08E-02	4.47E-02	45	0	0	55	45.41	1.70	0.89	51.98
16	6.20E-02	4.13E-02	65	0	0	35	61.06	−0.68	4.51	35.10
17	5.59E-02	3.90E-02	80	0	0	20	77.07	−1.48	3.05	21.35
18	8.03E-02	4.78E-02	0	5	95	0	−0.01	3.09	88.79	8.12
19	7.56E-02	4.62E-02	0	25	75	0	1.75	26.08	69.57	2.58
20	7.24E-02	4.52E-02	0	40	60	0	0.14	40.13	60.21	−0.49
21	6.92E-02	4.43E-02	0	55	45	0	−1.33	56.03	40.76	4.53
22	6.62E-02	4.35E-02	0	70	30	0	−1.96	71.72	32.44	−2.20
23	6.23E-02	4.22E-02	0	90	10	0	−0.27	91.86	5.81	2.58
24	9.17E-02	5.20E-02	0	10	0	90	3.96	10.93	−4.88	89.99
25	8.36E-02	4.96E-02	0	30	0	70	−4.27	35.89	2.58	65.79
26	7.79E-02	4.79E-02	0	45	0	55	−7.54	45.42	2.26	59.85
27	7.27E-02	4.60E-02	0	60	0	40	−0.24	60.35	−3.70	43.60
28	6.64E-02	4.38E-02	0	80	0	20	2.86	76.02	4.02	17.08
29	6.19E-02	4.21E-02	0	95	0	5	0.18	93.97	1.741	4.09
30	9.30E-02	5.20E-02	0	0	20	80	−0.41	0.28	22.96	77.16
31	9.09E-02	5.15E-02	0	0	35	65	4.36	1.62	30.58	63.42
32	8.80E-02	5.03E-02	0	0	55	45	0.52	0.53	54.47	44.46
33	8.59E-02	4.96E-02	0	0	70	30	0.75	−0.35	64.79	34.80
34	8.29E-02	4.86E-02	0	0	90	10	−0.82	−1.29	86.42	15.69
35	8.23E-02	4.83E-02	0	0	95	5	−0.57	0.31	94.68	5.57

8) The efficiency of network was checked for each architecture using the defined error.
9) The best network with lowest error was saved.

The best structure has two hidden layers; 9 neurons in first hidden layer and 14 neurons in second hidden layer. The activation function of input and output layers was “purelin” and the activation function of both hidden layers was “tansig”. The number of epochs was 800.

Table 4
Performance of the developed model.

Output	MRE		RMSE		MAE	
	Train	Test	Train	Test	Train	Test
1	0.09	1.60	1.98	3.14	1.62	2.38
2	0.12	0.20	1.87	2.33	1.49	1.78
3	0.76	1.72	2.60	3.38	2.19	2.90

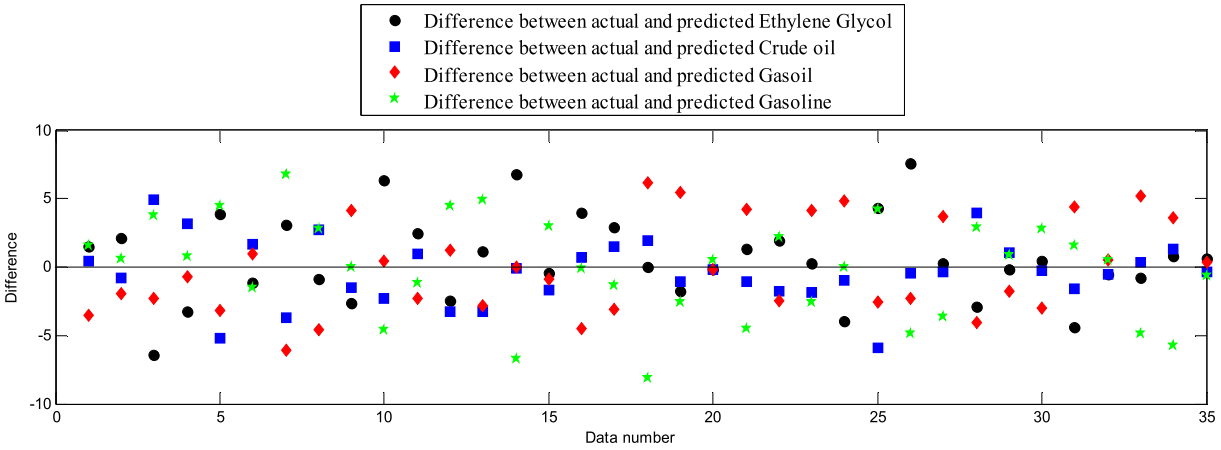

Fig. 5. The difference between actual and predicted values for test data.

3. Results and discussions

Regression diagrams of actual data defined in simulations and estimated data using presented MLP-LM model have been shown in Fig. 4. The good agreement between actual and predicted data is found clearly from this figure. In Table 3, the inputs, actual outputs and predicted outputs for test data have been tabulated. It should be noted that since the calculations in MCNP code are done per one particle emerged from the radiation source, the registered counts in the detector (as shown in 2nd and 3rd column in Table 3) are reported in decimal fractions (less than 1), whereas in real measurements they are integers. The difference between actual and predicted values for test data and for each output was shown in Fig. 5.

Mean Absolute Error (MAE), Mean Relative Error percentage (MRE %) and Root Mean Square Error (RMSE) of presented metering system are calculated by Equations (1)–(3).

$$MAE = \frac{1}{N}\sum_{i=1}^{Z}|X_i(Actual) - X_i(Measured)| \quad (1)$$

$$MRE\% = 100 \times \frac{1}{N}\sum_{i=1}^{N}\left|\frac{X_i(Actual) - X_i(Measured)}{X_i(Actual)}\right| \quad (2)$$

$$RMSE = \left[\frac{\sum_{i=1}^{N} X_i Actual\Big) - X_i(Measured))^2}{N}\right]^{0.5} \quad (3)$$

Performance of the developed model are indicated in Table 4 using Equations (1)–(3).

4. Conclusions

Information about the contents of transmission lines in oil, chemical and petrochemical industries especially in upstream oil industries is very important. Transmission of different fluids with different densities in a common line is often occurred. In this study, online monitoring of fluids was performed by determining type and amount of petroleum by-products. The proposed monitoring system was created by combination of dual energy densitometer and artificial intelligence. All of the simulations were performed using MATLAB software and MCNP code. A MLP-LM network with two inputs and three outputs was optimized using presented algorithm. Two features were extracted from detectors output signals and were considered as MLP-LM inputs. The trained network could meter the percentages of Ethylene Glycol, Crude oil, gasoil and gasoline based on input signals, precisely. The maximum RMSE of outputs was less than 3.4.

Declaration of competing interest

The authors declare that they have no known competing financial interests or personal relationships that could have appeared to influence the work reported in this paper.

References

[1] C.M. Salgado, L.E.B. Brandão, C.C. Conti, W.L. Salgado, Density prediction for petroleum and derivatives by gamma-ray attenuation and artificial neural networks, Appl. Radiat. Isot. 116 (2016) 143–149.

[2] A. Karami, G.H. Roshani, A. Khazaei, E. Nazemi, M. Fallahi, Investigation of different sources in order to optimize the nuclear metering system of gas–oil–water annular flows, Neural Comput. Appl. 32 (8) (2020) 3619–3631.

[3] D.F. Oliveira, R.S. Santos, A.S. Machado, A.S. Silva, M.J. Anjos, R.T. Lopes, Characterization of scale deposition in oil pipelines through X-Ray Microfluorescence and X-Ray microtomography, Appl. Radiat. Isot. 151 (2019) 247–255.

[4] S. Abdul-Majid, Determination of wax deposition and corrosion in pipelines by neutron back diffusion collimation and neutron capture gamma rays, Appl. Radiat. Isot. 74 (2013) 102–108.

[5] G.H. Roshani, E. Nazemi, A high performance gas–liquid two-phase flow meter based on gamma-ray attenuation and scattering, Nucl. Sci. Tech. 28 (11) (2017) 169.

[6] R. Hanus, L. Petryka, M. Zych, Velocity measurement of the liquid–solid flow in a vertical pipeline using gamma-ray absorption and weighted cross-correlation, Flow Meas. Instrum. 40 (2014) 58–63.

[7] V Mosorov, M Zych, R Hanus, D Sankowski, A Saoud, Improvement of flow velocity measurement algorithms based on correlation function and twin plane electrical capacitance tomography, Sensors 20 (1), 306.

[8] G.H. Roshani, E. Nazemi, M.M. Roshani, Flow regime independent volume fraction estimation in three-phase flows using dual-energy broad beam technique and artificial neural network, Neural Comput. Appl. 28 (1) (2017) 1265–1274.

[9] G.H. Roshani, S.A.H. Feghhi, A. Mahmoudi-Aznaveh, E. Nazemi, A. Adineh-Vand, Precise volume fraction prediction in oil–water–gas multiphase flows by means of gamma-ray attenuation and artificial neural networks using one detector, Measurement 51 (2014) 34–41.

[10] Robert Hanus, Marcin Zych, Maciej Kusy, Marek Jaszczur, Leszek Petryka, Identification of liquid-gas flow regime in a pipeline using gamma-ray absorption technique and computational intelligence methods, Flow Meas. Instrum. 60 (2018) 17–23.

[11] G.H. Roshani, E. Nazemi, M.M. Roshani, Usage of two transmitted detectors with optimized orientation in order to three phase flow metering, Measurement 100 (2017) 122–130.

[12] V Mosorov, Improving the accuracy of single radioactive particle technique for flow velocity measurements, Flow Meas. Instrum. 66, 150-156.

[13] C.M. Salgado, C.M.N.A. Pereira, R. Schirru, L.E.B. Brandao, Flow regime identification and volume fraction prediction in multiphase flows by means of gamma-ray attenuation and artificial neural networks, Prog. Nucl. Energy 52 (2010) 555–562.

[14] M. Khorsandi, S.A.H. Feghhi, Design and construction of a prototype gamma-ray densitometer for petroleum products monitoring applications, Measurement 44 (9) (2011) 1512–1515.

[15] G.H. Roshani, S.A.H. Feghhi, A. Adineh-Vand, M. Khorsandi, Application of adaptive neuro-fuzzy inference system in prediction of fluid density for a gamma ray densitometer in petroleum products monitoring, Measurement 46 (9) (2013) 3276–3281.

[16] W.L. Salgado, R.S.D.F. Dam, C.M. Barbosa, A.X. da Silva, C.M. Salgado, Monitoring system of oil by-products interface in pipelines using the gamma radiation attenuation, Appl. Radiat. Isot. (2020) 109125.

[17] D.B. Pelowitz, MCNP-X TM User's Manual, Los Alamos National Laboratory, 2005. Version 2.5.0. LA-CP-05e0369.

[18] E. Nazemi, G.H. Roshani, S.A.H. Feghhi, S. Setayeshi, E. Eftekhari Zadeh, A. Fatehi, Optimization of a method for identifying the flow regime and measuring void fraction in a broad beam gamma-ray attenuation technique, Int. J. Hydrogen Energy 41 (2016) 7438–7444.

[19] E. Nazemi, G.H. Roshani, S.A.H. Feghhi, R. Gholipour Peyvandi, S. Setayeshi, Precise void fraction measurement in two-phase flows independent of the flow regime using gamma-ray attenuation, Nucl. Eng. Technol. 48 (2016) 64–71.

[20] G.H. Roshani, E. Nazemi, S.A.H. Feghhi, S. Setayeshi, Flow regime identification and void fraction prediction in two-phase flows based on gamma ray attenuation, Measurement 62 (2015) 25–32.

[21] G.H. Roshani, E. Nazemi, S.A.H. Feghhi, Investigation of using 60Co source and one detector for determining the flow regime and void fraction in gas-liquid two-phase flows, Flow Meas. Instrum. 50 (2016) 73–79.

[22] R.J. McConn, C.J. Gesh, R.T. Pagh, R.A. Rucker, R. Williams III, Compendium of Material Composition Data for Radiation Transport Modeling (No. PNNL-15870 Rev. 1). Pacific Northwest National Lab.(PNNL), 2011. Richland, WA (United States).